



- Author(s)** Raitoharju, Matti; Nurminen, Henri; Piché, Robert
- Title** A linear state model for PDR+WLAN positioning
- Citation** Raitoharju, Matti; Nurminen, Henri; Piché, Robert 2013. A linear state model for PDR+WLAN positioning. In: Morawiec, Adam; Hinderscheit, Jinnie (ed.). Proceedings of the 2013 Conference on Design and Architectures for Signal and Image Processing DASIP Cagliari, Italy, October 8-10, 2013. Conference on Design and Architectures for Signal and Image Processing Belmont France, European Electronic Chips & Systems Design Initiative (ECSI) . 113-118.
- Year** 2013
- DOI**
- Version** Post-print
- URN** <http://URN.fi/URN:NBN:fi:ty-201403051119>
- Copyright** © 2013 IEEE. Personal use of this material is permitted. Permission from IEEE must be obtained for all other uses, in any current or future media, including reprinting/republishing this material for advertising or promotional purposes, creating new collective works, for resale or redistribution to servers or lists, or reuse of any copyrighted component of this work in other works.

A Linear State Model for PDR+WLAN Positioning

Matti Raitoharju, Henri Nurminen and Robert Piché

Department of Automation Science and Engineering

Tampere University of Technology

P.O. Box 692, FI-33101 Tampere, Finland

E-mail addresses: firstname.lastname@tut.fi

Abstract—Indoor positioning based on WLAN signals is often enhanced using pedestrian dead reckoning (PDR) based on an inertial measurement unit. The state evolution model in PDR is usually nonlinear. We present a new linear state evolution model for PDR. In simulated-data and real-data tests of tightly coupled WLAN-PDR positioning, we find that the positioning accuracy with this linear model is almost as good as with traditional models when the initial state is known, and better when the initial state is not known. The proposed method is computationally light and is also suitable for smoothing.

Keywords—Sensor based localization, Hybridization approaches, Signals-of-Opportunity, Pedestrian dead reckoning

I. INTRODUCTION

Wireless Local Area Network (WLAN) access points (APs) are numerous and ubiquitous in most indoor environments. Although WLAN is meant for data transfer, the WLAN signals may be used for user localization. Because the WLAN APs are not meant for positioning, they do not usually send information on their own location for clients. WLAN positioning therefore makes use of a “radio map”, which describes certain features of the WLAN signal characteristics at given locations. A radio map is created and updated using data collected on site. These data are called fingerprints (FP). A FP is a report that contains at least the receiver location and the IDs and the received signal strength (RSS) values of APs within reception range. A radio map is constructed off-line based on the collected FPs. The accuracy of positioning based on WLAN signals depends on the model and environment. In small scale (a few buildings) it is possible to achieve positioning results of the order of a couple of meters [1]. For large scale positioning (a city or larger) when the size of the database is a limiting factor the positioning accuracy can be of the order of tens of meters [2].

Pedestrian dead reckoning (PDR) uses an inertial measurement unit (IMU) to detect when a user takes footsteps and how the direction changes between footsteps. The IMU has three axis accelerometers and gyroscopes. The user heading change is computed by projecting the gyroscope measurements to the horizontal plane which is estimated from the accelerometer [3]. The footstep length may also be estimated from the IMU data. If the sensor is mounted on the foot, it is possible to detect when the foot is still and then integrate the footstep length from the IMU data [4]. If the IMU is handheld the footstep length can be inferred from the IMU data also by other methods, see for example [5, 6]. A PDR system can greatly improve the positioning locally as the position estimate may be updated every footstep, but because the errors accumulate over time

PDR is often combined with other sensors that can, at least occasionally, provide information of the absolute position.

In this paper we investigate models for fusing PDR measurements with WLAN measurements. We propose a linear state model for the state evolution, whereas in the literature the state model used with PDR system is usually nonlinear [6–8]. For nonlinear estimation in general there is no closed form optimal algorithm. In this paper we use Kalman and Extended Kalman filters, which are computationally light algorithms.

Section II contains the filtering and smoothing algorithms that are used to estimate the user’s kinematic state. In Section III we present the WLAN model that is used for positioning. The evaluated PDR models are presented in Section IV. In Section V we evaluate the performance of different models with real and simulated data and Section VI concludes the paper.

II. FILTERING ALGORITHMS

The Kalman filter is an algorithm for estimating the state of the system given a time-series of measurements in the case of linear state-evolution and measurement models. If the measurements and state transitions are also normally distributed, the Kalman filter is optimal. The algorithm uses the following update equations at each time index t [9]

$$x_{t|t-1} = F_t x_{t-1|t-1} \quad (1)$$

$$P_{t|t-1} = F_t P_{t-1|t-1} F_t^T + Q_t \quad (2)$$

$$S_t = H_t P_{t|t-1} H_t^T + R_t \quad (3)$$

$$K_t = P_{t|t-1} H_t^T S_t^{-1} \quad (4)$$

$$x_{t|t} = x_{t|t-1} + K_t (y_t - H_t x_{t|t-1}) \quad (5)$$

$$P_{t|t} = (I - K_t H_t) P_{t|t-1}, \quad (6)$$

where x is the state vector, P is the state covariance matrix, F is the state transition matrix, Q is the state transition error covariance matrix, R is the measurement error covariance matrix and

$$y_t = H_t x_t \quad (7)$$

is the linear measurement equation. If the state model is nonlinear then (1) has to be replaced with

$$x_{t|t-1} = f(x_{t-1|t-1}) \quad (8)$$

and F_t in (2) with

$$F_t = \frac{\partial f(x_{t-1|t-1})}{\partial x_{t-1|t-1}}, \quad (9)$$

to get the approximative nonlinear estimation algorithm known as the Extended Kalman filter (EKF) [10].

The Rauch-Tung-Striebel smoother [11] may be used to enhance the state estimates when measurements of future time instants can also be used, for example when plotting the track over a given time interval. The recursive smoothing equations are

$$C_t = P_{t|t} F_t^T P_{t+1|t}^{-1} \quad (10)$$

$$x_{t|m} = x_{t|t} + C_t(x_{t+1|m} - x_{t+1|t}) \quad (11)$$

$$P_{t|m} = P_{t|t} + C_t(P_{t+1|m} - P_{t+1|t})C_t^T, \quad (12)$$

where m is the last time index.

III. COVERAGE AREA POSITIONING

In its simplest form, probabilistic coverage area (CA) positioning is a method for radio map construction in which the reception area of each AP is modeled as a two-dimensional normal distribution. The radio map does not contain any raw RSS data, and thus computational, memory and communication complexity is much lower compared to conventional FP positioning methods. The algorithm and derivations are explained in [12] and here we only briefly present the algorithm.

The coverage area estimate is

$$\mu_n = \frac{\sum z_i}{n} \quad (13)$$

$$\Sigma_n = \frac{\sum z_i z_i^T + B - n\mu_n \mu_n^T}{n+1}, \quad (14)$$

where μ_n and Σ_n are the mean and covariance of the CA estimate based on n FPs, z_i is the location of the i^{th} FP and B is the prior covariance.

When a new measurement is received, these parameters may be updated by

$$\mu_{n+1} = \frac{n\mu_n + z_{n+1}}{n+1} \quad (15)$$

$$\Sigma_{n+1} = \frac{(n+1)(\Sigma_n - \mu_{n+1}\mu_{n+1}^T) + z_{n+1}z_{n+1}^T + n\mu_n\mu_n^T}{n+2} \quad (16)$$

Because the AP models are linear-Gaussian they may be used in KF directly with

$$y = \mu \quad (17)$$

$$H = [I \quad 0] \quad (18)$$

$$R = \Sigma. \quad (19)$$

Here for H it is assumed that the first variables in the state are the position variables.

IV. PEDESTRIAN DEAD RECKONING

In most of the literature, the state model used in PDR is nonlinear [6–8]. For comparison purposes, we consider two traditional models. In the first one, the state contains the user location and the direction of movement

$$x_{t|t-1} = \begin{bmatrix} r_{1,t} \\ r_{2,t} \\ \theta_t \end{bmatrix} = \begin{bmatrix} r_{1,t-1} + s_t \cos \theta_{t-1} \\ r_{2,t-1} + s_t \sin \theta_{t-1} \\ \theta_{t-1} + \Delta \theta_t \end{bmatrix}, \quad (20)$$

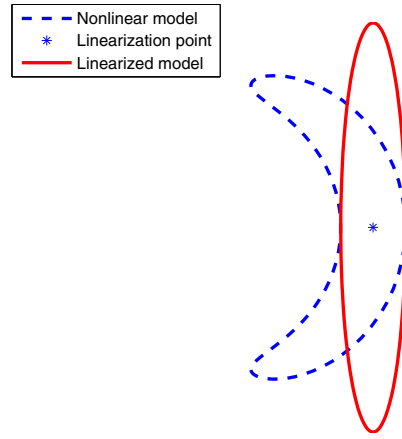


Figure 1. Footstep propagation with nonlinear and linearized state models

where $\Delta \theta_t$ is the change of heading obtained from gyroscopes and s_t is the footstep length estimated from accelerometer data. The linearized state transition matrix is

$$F_t = \begin{bmatrix} 1 & 0 & -s_t \sin \theta_{t-1} \\ 0 & 1 & s_t \cos \theta_{t-1} \\ 0 & 0 & 1 \end{bmatrix}. \quad (21)$$

and the linearized state transition noise covariance is

$$Q_t = \begin{bmatrix} \sigma_s^2 \cos^2 \theta_{t-1} & 0 & 0 \\ 0 & \sigma_s^2 \sin^2 \theta_{t-1} & 0 \\ 0 & 0 & \sigma_{\Delta \theta}^2 \end{bmatrix}. \quad (22)$$

In our second traditional model the footstep length is also estimated:

$$x_{t|t-1} = \begin{bmatrix} r_{1,t} \\ r_{2,t} \\ \theta_t \\ s_t \end{bmatrix} = \begin{bmatrix} r_{1,t-1} + s_{t-1} \cos \theta_{t-1} \\ r_{2,t-1} + s_{t-1} \sin \theta_{t-1} \\ \theta_{t-1} + \Delta \theta_t \\ s_{t-1} \end{bmatrix}, \quad (23)$$

$$F_t = \begin{bmatrix} 1 & 0 & -s_{t-1} \sin \theta_{t-1} & \cos \theta_{t-1} \\ 0 & 1 & s_{t-1} \cos \theta_{t-1} & \sin \theta_{t-1} \\ 0 & 0 & 1 & 0 \\ 0 & 0 & 0 & 1 \end{bmatrix} \quad (24)$$

and

$$Q_t = \begin{bmatrix} 0 & 0 & 0 & 0 \\ 0 & 0 & 0 & 0 \\ 0 & 0 & \sigma_{\Delta \theta}^2 & 0 \\ 0 & 0 & 0 & \sigma_{\Delta s}^2 \end{bmatrix}. \quad (25)$$

Figure 1 shows position estimates after taking one footstep from known position using this model. The dashed line shows how the state is propagated if the original nonlinear model is used and the solid line shows the linearized state.

We propose the linear state model

$$x_{t|t-1} = \begin{bmatrix} r_{1,t} \\ r_{2,t} \\ v_{1,t} \\ v_{2,t} \end{bmatrix} = \begin{bmatrix} 1 & 0 & 1 & 0 \\ 0 & 1 & 0 & 1 \\ 0 & 0 & \cos \Delta \theta_t & -\sin \Delta \theta_t \\ 0 & 0 & \sin \Delta \theta_t & \cos \Delta \theta_t \end{bmatrix} \begin{bmatrix} r_{1,t-1} \\ r_{2,t-1} \\ v_{1,t-1} \\ v_{2,t-1} \end{bmatrix} = F_t x_{t-1|t-1} \quad (26)$$

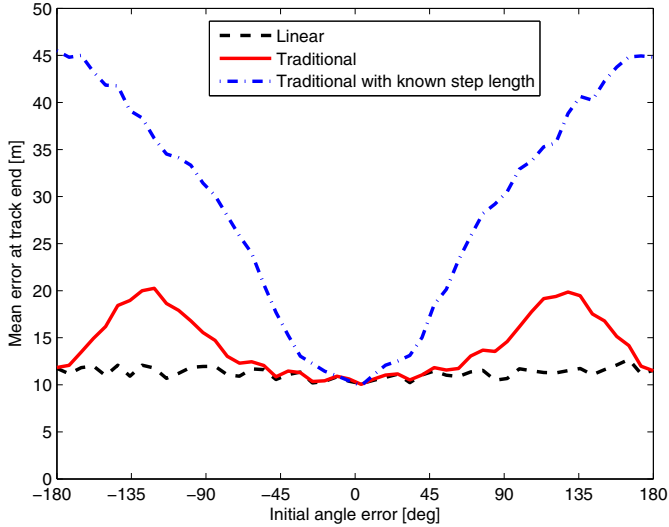


Figure 2. Mean of errors at track end as the function of initial direction estimate

where v is the footstep vector estimate. The process noise covariance matrix is

$$Q_t = \begin{bmatrix} 0 & 0 & 0 & 0 \\ 0 & 0 & 0 & 0 \\ 0 & 0 & \sigma_v^2 & 0 \\ 0 & 0 & 0 & \sigma_v^2 \end{bmatrix}. \quad (27)$$

Compared to the traditional models the proposed model has the benefit that the state transition matrix and the state transition covariance matrix are independent of the state. To keep those independent of the state estimate the state transition error cannot have different variances for heading and footstep length.

V. PERFORMANCE EVALUATION

A. Simulated Tests

In simulations we tested how the linear model performs against the traditional models when the data is generated using the traditional model. For the first simulation, the state model is such that the standard deviations of footstep length is $\sigma_{\Delta s} = 0.01$ m and for the heading change is $\sigma_{\Delta\theta} = \frac{0.01}{0.7}$ rad. The initial footstep length is set to 0.7 m. If the footstep length does not change much during the track, the linear model, where $\sigma_v = 0.01$ m, has same amount of propagated error in position. The simulated test track is 50 footsteps and at every time step there is a 10% probability of receiving a location measurement with variance $10^2 \text{ m}^2 I$. Initial covariance variance for location dimensions is 10^2 m^2 and for rest of variables $\sigma_{s_0} = 1$ m, $\sigma_\theta = \frac{1}{0.7}$ rad and $\sigma_{v_0} = 1$ m.

Figure 2 shows the position errors of the last time step as a function of initial state heading error. Methods tested are the linear and traditional models that estimate both the heading and the footstep length and also the traditional model that gets accurate footstep lengths. From the figure we can see that the linear and traditional models are almost equally accurate when the angle error is small. On the other hand the method

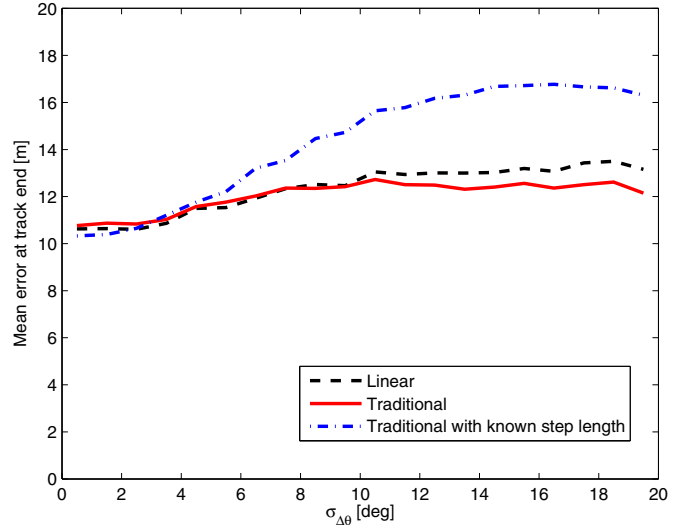


Figure 3. Mean of errors at track end as the function of heading change error

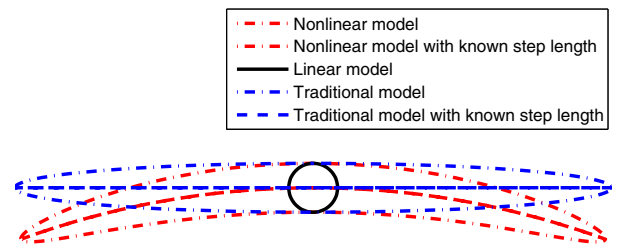


Figure 4. Model errors when $\sigma_{\Delta\theta} = 10$ deg

with footstep length information works badly when the initial heading error is large. The reason why the traditional method with footstep length estimation is again good when the angle approaches 180 degrees is that the footstep length estimate is equivalent to the negative value of the estimate for 0 degrees.

In Figure 3 we investigate how the different methods perform when the heading error (i.e. gyroscope accuracy) is changed. The traditional models have the correct σ_θ and σ_s , but the linear model is the same as in the first tests because we want to keep the variance independent of the user state. For this test the initial heading is accurate.

From the figure we see that if the heading error is small, the traditional method with accurate footstep length estimates has similar accuracy as the proposed method, but when the angular error grows the model performs badly. The proposed method performs somewhat worse than the traditional method when the variance in angular direction is large, but slightly better when it is small.

Figure 4 shows what kind of error estimates the different methods produce when the $\sigma_{\Delta\theta} = 10$ deg. At this point there is not significant accuracy difference between the proposed and traditional method. This shows how the error can be quite asymmetric before the linear model has worse accuracy than the traditional model. The figure also shows the difference

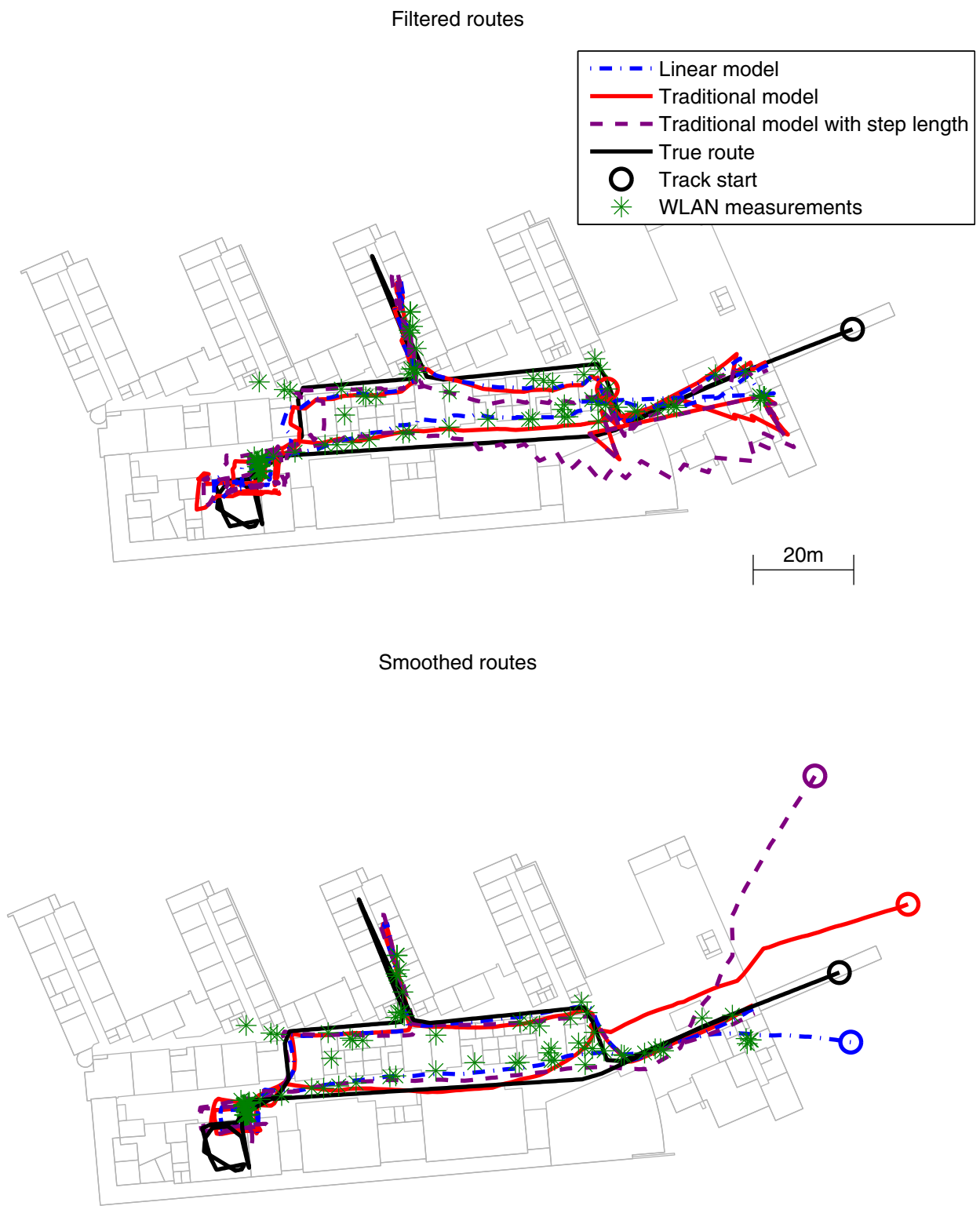


Figure 5. Estimated routes with different models

between the traditional model with known footstep length and how the error would be without linearization. The poor accuracy of the traditional model with known footstep length is caused by the linearization error, which is not taken into account in the model error.

B. True Data

In the true data test the algorithm is tested in one floor of a building in the Tampere University of Technology. The radio map of the test floor contains approximately 200 WLAN APs. The measurements were collected using a XSENS MTi IMU and Acer Iconia tablet. Both devices were carried in hand while doing measurements.

For the WLAN positioning we use the two-level coverage area method proposed in [13]. We generate two coverage areas: a weak CA that is constructed using all FPs, and a strong CA that is constructed with only FPs that have signal strength $\geq -70\text{dBm}$. The prior for weak CA is $B = 1000^2 \text{m}^2 I$ and for strong CA $B = 5^2 \text{m}^2 I$. According to [13] the two-level normal CA models have around 10% larger errors than traditional location fingerprinting, but require only storage of 10 parameters for each AP. Also, the measurements can be used as linear measurements in the Kalman filter.

Figure 5 shows filtered and smoothed tracks. The initial heading for traditional models is 90 degrees off and the initial footstep length estimate of the traditional model is 0.8 m. The traditional method is tested also with step lengths estimated from the sensor data with $\sigma_s = 0.3\text{m}$. For the linear model the initial footstep vector is $\mathbf{0}$ with variance $1 \text{m}^2 I$. The initial position variance is large i.e. the prior is almost uninformative. The smoothed routes have quite big difference in the right hand side of the picture, where the route began. The traditional models are more off than the linear model. This is caused from the wrong linearization of the F matrix in the beginning of the track. The smoothing was done using these F matrices in (10); better results might be obtained with more complex methods such as the Unscented Rauch-Tung-Striebel smoother [14].

Some error statistics are given in Table I. In the table θ_0 is the initial error on the heading. ‘‘Static’’ denotes the WLAN-only position estimates without filtering. When there is only footstep measurements without WLAN measurements, the ‘‘Static’’ uses the last position computed from WLAN measurements as the position estimate. When filtering the proposed method has the best accuracy except when the traditional methods are initialized with the correct initial heading. In smoothing the traditional method with footsteps estimated from sensor data has a slightly better accuracy also when the initial heading is 45 degrees off. The more the initial heading error is the worse the accuracy of traditional methods get. When the initial heading is 180 degrees off neither of traditional methods improve ‘‘Static’’ estimates and the traditional model without footstep lengths from sensor data has even larger errors than ‘‘Static’’.

Footstep length approximations given by different methods are shown in Figure 6. The footstep lengths are computed in the case shown in Figure 5 ($\theta_0 = 90^\circ$). Here we see that the footstep length estimated with the traditional model (s) and the proposed linear model ($\|v\|$) are rather different in the beginning of the track, but become similar towards the end

Table I. MEAN ERRORS [m] OF DIFFERENT METHODS AND DIFFERENT INITIAL HEADING ERRORS

Method	θ_0	Filtered	Smoothed
Traditional w footstep length	0°	6.7	3.8
Traditional w/o footstep length	0°	7.4	4.3
Traditional w footstep length	45°	7.3	4.3
Traditional w/o footstep length	45°	9.2	5.1
Traditional w footstep length	90°	7.4	5.2
Traditional w/o footstep length	90°	10.7	6.9
Traditional w footstep length	135°	7.5	6.1
Traditional w/o footstep length	135°	13.4	9.7
Traditional w footstep length	180°	8.2	7.3
Traditional w/o footstep length	180°	12.1	8.0
Linear		6.8	4.6
Static		8.2	

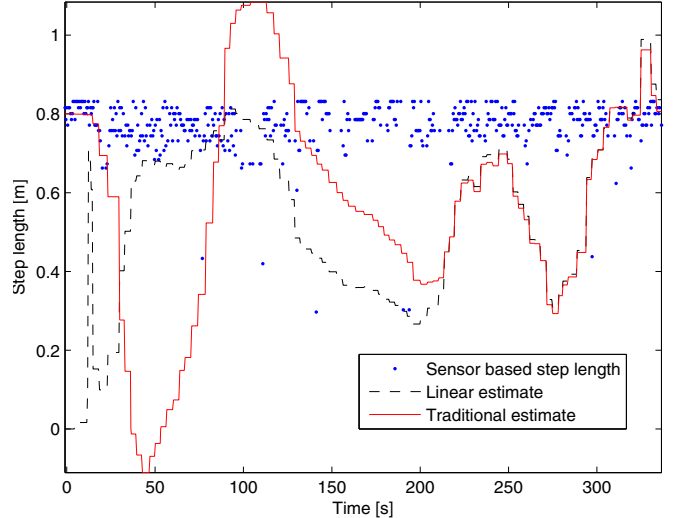


Figure 6. Footstep length estimates

of the track. From 40s to 120s the linear step length is rather constant whereas the estimates computed using the traditional model varies from -0.1m to 1.1m . In the middle of the route the footstep length estimates are shorter than the footsteps were in reality. This is caused by the WLAN estimates in lower left part of the Figure 5 that are all in same location whereas the true route goes around the lecture hall.

VI. CONCLUSIONS

We proposed in this paper a novel linear model for PDR in indoor personal positioning and compared it to models that are common in the literature. The evaluation shows that although the model is simpler than the traditional methods it performs well and is especially suited for situations where the initial heading and position are not known. As the proposed model is linear it can also be smoothed with the Rauch-Tung-Striebel smoother.

ACKNOWLEDGEMENTS

This work was supported by Tampere Doctoral Programme in Information Science and Engineering, Nokia inc., Nokia Foundation and Jenny and Antti Wihuri Foundation. The authors want to thank Jussi Collin and Jussi Parviainen for codes that estimate the footsteps and headings from the sensor data.

REFERENCES

- [1] C. Rizos, A. G. Dempster, B. Li, and J. Salter, "Indoor positioning techniques based on wireless LAN," in *AusWireless '06, Sydney, Australia*, March 2006.
- [2] Y.-C. Cheng, Y. Chawathe, A. LaMarca, and J. Krumm, "Accuracy characterization for metropolitan-scale Wi-Fi localization," in *Proceedings of the 3rd International Conference on Mobile systems, Applications, and Services*, ser. MobiSys '05. New York, NY, USA: ACM, 2005, pp. 233–245.
- [3] J. Collin, O. Mezentsev, and G. Lachapelle, "Indoor positioning system using accelerometry and high accuracy heading sensors," in *Proceedings of the ION GPS/GNSS 2003 Conference*, 2003, pp. 9–12.
- [4] S. Beauregard, "Omnidirectional Pedestrian Navigation for First Responders," in *4th Workshop on Positioning, Navigation and Communication, 2007. (WPNC '07)*, 2007, pp. 33–36.
- [5] S. H. Shin, C. Park, J. W. Kim, H. Hong, and J. M. Lee, "Adaptive Step Length Estimation Algorithm Using Low-Cost MEMS Inertial Sensors," in *Sensors Applications Symposium, 2007. SAS '07. IEEE*, 2007, pp. 1–5.
- [6] H. Leppäkoski, J. Collin, and J. Takala, "Pedestrian navigation based on inertial sensors, indoor map, and WLAN signals," in *IEEE International Conference on Acoustics, Speech and Signal Processing (ICASSP), 2012*, 2012, pp. 1569–1572.
- [7] R. Jirawimut, P. Ptasinski, V. Garaj, F. Cecelja, and W. Balachandran, "A method for dead reckoning parameter correction in pedestrian navigation system," *IEEE Transactions on Instrumentation and Measurement*, vol. 52, no. 1, pp. 209–215, 2003.
- [8] F. Evennou and F. Marx, "Advanced integration of WiFi and inertial navigation systems for indoor mobile positioning," *Eurasip Journal on Applied Signal Processing*, vol. 2006, pp. 164–164, 2006.
- [9] Y. Ho and R. Lee, "A Bayesian approach to problems in stochastic estimation and control," *IEEE Transactions on Automatic Control*, vol. 9, no. 4, pp. 333 – 339, oct 1964.
- [10] A. Gelb, *Applied optimal estimation*. MIT Press, 1974.
- [11] H. E. Rauch, C. Striebel, and F. Tung, "Maximum likelihood estimates of linear dynamic systems," *AIAA Journal*, vol. 3, no. 8, pp. 1445–1450, 1965.
- [12] L. Koski, R. Piché, V. Kaseva, S. Ali-Löytty, and M. Hännikäinen, "Positioning with coverage area estimates generated from location fingerprints," in *7th Workshop on Positioning Navigation and Communication (WPNC)*, 2010, pp. 99–106.
- [13] M. Raitoharju, M. Dashti, S. Ali-Löytty, and R. Piché, "Positioning with multilevel coverage area models," in *2012 International Conference on Indoor Positioning and Indoor Navigation (IPIN2012)*, November 2012.
- [14] S. Särkkä, "Unscented rauch–tung–striebel smoother," *Automatic Control, IEEE Transactions on*, vol. 53, no. 3, pp. 845–849, 2008.